

Size-dependent magnetic properties of Ni/C₆₀ granular films

Zhijun Zhao,¹ Haiqian Wang,¹ Bing Wang,¹ and J. G. Hou^{1,2,*}

¹Structure Research Lab, University of Science and Technology of China, Hefei 230026, Anhui, Peoples Republic of China

²International Center for Quantum Structures, Chinese Academy of Sciences, Beijing 100080, Peoples Republic of China

G. L. Liu and X. F. Jin

Surface Physics Laboratory, Fudan University, Shanghai 200433, People's Republic of China

(Received 11 November 2001; published 28 May 2002)

Ni/C₆₀ granular films were prepared by magnetron sputtering and thermal evaporation techniques with different ratios of Ni atoms to C₆₀ molecules. A high-resolution transmission microscopy analysis shows that Ni nanoparticles are well isolated and embedded in an amorphous C₆₀ matrix. X-ray-diffraction and Raman spectra indicate lattice expansion of Ni particles and charge transfer from Ni to C₆₀, which provide clear evidence that strong interfacial interactions exist between Ni particles and the C₆₀ matrix. Measurements of the surface magneto-optical Kerr effect show that the coercivities (H_C) of Ni particles embedded in C₆₀ matrix are enhanced significantly. The film with an average Ni particle size of 3.3 nm still presents ferromagnetism with a value of H_C of 45 Oe at room temperature. We suggest that the enhancement of H_C may be attributed to surface spin disorder of Ni particles induced by the strong interfacial interaction between Ni and C₆₀.

DOI: 10.1103/PhysRevB.65.235413

PACS number(s): 75.50.Tt, 75.70.Cn, 61.48.+c

I. INTRODUCTION

Many researchers have given evidence of interfacial interactions between C₆₀ and metals, e.g., charge transfer and surface reconstruction.^{1,2} The charge transfer from metal to C₆₀ may provide opportunities to find interesting properties in metal/C₆₀ nanocomposite materials, since the interfacial atomic and electronic structures are very important to the properties of nanostructured materials.³⁻⁵ Based on this consideration, some interesting physical and structural properties of (Co,Fe,CoFe)/C₆₀,⁶ Ag/C₆₀ nanocomposite films⁷ and (Al,Cu)/C₆₀ multilayer films⁸ have already been reported.

It is known that the interaction between C₆₀ and Ni is strong. When C₆₀ was deposited on Ni(110), reconstruction of the Ni(110) surface was induced and ~ 2 electrons were transferred from Ni to C₆₀.⁹ Therefore, it is reasonable to expect that the magnetic properties of the Ni nanoparticles embedded in the C₆₀ matrix will be different from that of Ni/SiO₂ nanocomposite or graphite-coated magnetic nanocrystalline films which were studied intensively in the past years.¹⁰⁻¹⁴

Understanding the magnetic properties of nanoparticles is a central issue in magnetic materials.¹⁵ In many cases, finite-size effects dominate the magnetic properties of nanoparticles, and become more important as the particle size decreases because of the competition between surface magnetic properties and core magnetic properties.¹⁶ For a particle of radius ~ 4 nm, 50% of atoms lie on the surface. The symmetry breaking at the surface results in a surface anisotropy. In other cases, the magnetic properties of nanoparticles are strongly influenced when the surface is in contact with different media.¹⁷ Therefore, surface effects in a nanoparticle are of great important.

In this paper, we report our studies on the preparation and characterization of Ni/C₆₀ granular films with Ni nanoparticles embedded in amorphous C₆₀ matrix. We find that the coercivity of Ni nanoparticles is enhanced significantly, and

the critical size for the superparamagnetic transition is about 3 nm, which is remarkably smaller than that of Ni embedded in SiO₂ or graphite matrix.^{11,13,14}

II. EXPERIMENT

Granular Ni/C₆₀ films were prepared in a magnetron sputtering system. The base pressure was $\sim 2.0 \times 10^{-5}$ Pa. High-purity argon gas (99.999%) was used as the sputtering gas. The Ni target (99.99%) was sputtered with dc magnetron sputtering at a pressure of 3.0 Pa, and the deposition rate was ~ 0.15 nm/sec. A thermal heating source was used to sublimate C₆₀ powder (99.9%) at a deposition rate of ~ 0.06 nm/sec. The Ni target and the C₆₀ heating source were separated from each other. During deposition, a substrate (SiO₂ glass, Si, or NaCl) was placed on a disk and was exposed alternatively to the two sources controlled by a computer. In order to obtain homogeneous Ni/C₆₀ composite films, the holding time of the substrate under each source was limited so that the deposition thickness in each cycle is less than 1 ML. In this way, the two components can blend into each other very well. Five samples with various nominal ratios of Ni atoms to C₆₀ molecules ($N_{Ni}:N_{C60}$) from 1.5 to 30 were prepared by adjusting the holding times under Ni and C₆₀ sources.

Films on SiO₂ glass substrates with a nominal thickness of 50 nm were analyzed by x-ray diffractometry (XRD) with 18-kW Cu $K\alpha$ radiation. Films with a nominal thickness of 25 nm were also deposited on freshly cleaved NaCl(001) substrates for JEOL 2010 high-resolution transmission electron microscopy (HRTEM) analysis. A Raman spectrometer was used to investigate the metal/C₆₀ interfacial interactions in films on Si substrates with nominal thickness of 200 nm. Magnetic properties of the films on SiO₂ substrates were measured by a surface magneto-optical Kerr effect (SMOKE) measurement system at room temperature. The dc magnetic field was applied in an in-plane direction in a scanning range from -2 to 2 kOe.

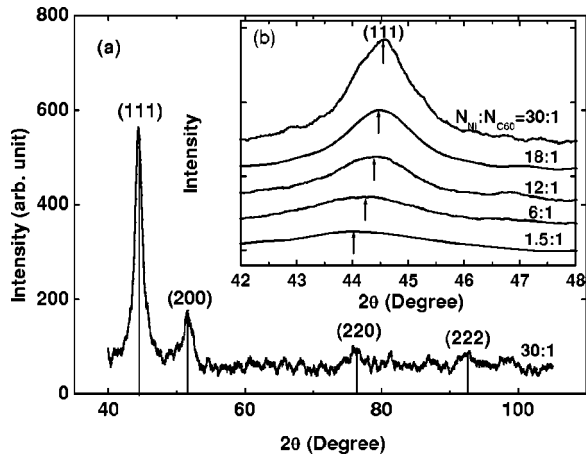


FIG. 1. The spectra of x-ray diffraction at room temperature. (a). The spectrum of the film in which $N_{Ni}:N_{C60}=30$ is in the scanning range of 40° – 105° . (b) Ni (111) XRD peaks of the films. The arrows indicate the Ni(111) peak positions.

III. RESULTS AND DISCUSSION

Figure 1(a) shows a typical XRD spectrum of the as-deposited $N_{Ni}:N_{C60}=30$ film on glass substrates in a 2θ scanning range of 40° – 105° . Because the XRD peak positions and the relative intensities of the samples match those of polycrystalline Ni powder, we conclude that there is no dominant crystalline orientation for the Ni grains. Therefore, we can calculate the average diameters of Ni grains with the Scherrer relation. The results show that the average size decreases from 6.6 to 2.6 nm as the $N_{Ni}:N_{C60}$ ratio decreases from 30:1 to 1.5:1 (see Table I). At the same time, the Ni(111) peak position downshifts from 44.5° to 44.0° [Fig. 1(b)], indicating that the lattice of the Ni particles expands, and the expansion increases with the decrease of particle size. For example, the identity distance of Ni(111) for a 6.6-nm particle ($N_{Ni}:N_{C60}=30$) is 2.036 \AA and that for a 2.6-nm particle ($N_{Ni}:N_{C60}=1.5$) is 2.056 \AA , while the bulk value is 2.034 \AA .

A typical HRTEM image of an as-deposited Ni/ C_{60} granular film ($N_{Ni}:N_{C60}=6$) is shown in Fig. 2. From this figure, we can see that Ni nanoparticles are embedded in an amorphous C_{60} matrix. The statistical result of the particle size obtained by counting over hundreds of particles is displayed in the inset of Fig. 2, which indicates that the size distribution is narrow and the average size is ~ 3.2 nm. This consists with the XRD result (3.3 nm). We also estimated from HR-

TABLE I. Structure parameters and coercivity (H_C) of the Ni/ C_{60} films. D is the average size of Ni particles, d_{Ni} is the identity distance of Ni (111), and H_C is the coercivity of Ni particles.

No.	$N_{Ni}:N_{C60}$	D (nm)	d_{Ni} (\AA)	H_C (Oe)
1	1.5:1	2.6	2.056	~ 0
2	6:1	3.3	2.052	45
3	12:1	4.3	2.046	47
4	18:1	5.1	2.039	66
5	30:1	6.6	2.036	85

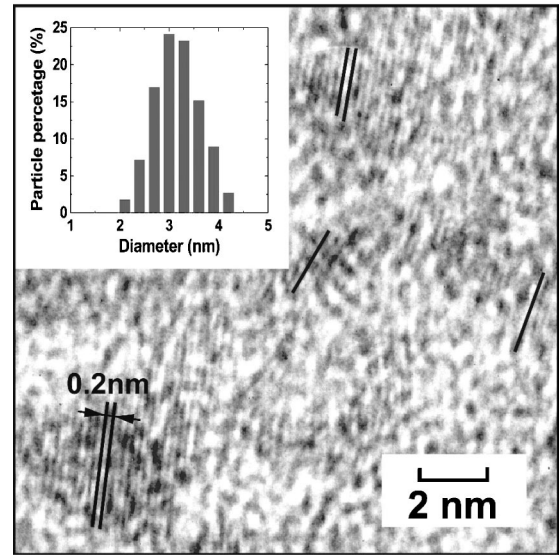


FIG. 2. The HRTEM image of the film ($N_{Ni}:N_{C60}=6$). The black lines are guides to the eye for the Ni(111) lattice.

TEM images that the average interparticle separation of Ni nanoparticles is 2.5 nm.

Figure 3 shows the Raman spectra of the Ni/ C_{60} films with $N_{Ni}:N_{C60}$ ratios of 1.5, 6, and 30 respectively. The measurements were performed at room temperature, and the laser power was below 50 mW/cm^2 in order to minimize the possible photopolymerization effect of C_{60} molecules. The peak at 1469 cm^{-1} corresponds to the pentagonal pinch mode [Ag(2) in pristine C_{60}]. The peaks at 1457 cm^{-1} ($N_{Ni}:N_{C60}=1.5$ and 6) and 1444 cm^{-1} ($N_{Ni}:N_{C60}=30$) are the “soften” modes of Ag(2); they reflect the charge transfer from Ni to C_{60} . The downshift of the Ag(2) mode in an $N_{Ni}:N_{C60}=30$ film is 25 cm^{-1} , and that in $N_{Ni}:N_{C60}=1.5$ and 6 films is 12 cm^{-1} . According to the calibration of the 6-cm^{-1} downshift of the Ag(2) mode per electron transfer,¹⁸ we derived that the charge transferred to each C_{60} molecule in an $N_{Ni}:N_{C60}=30$ film is ~ 4 electrons, and that in $N_{Ni}:N_{C60}=1.5$ and 6 films are ~ 2 electrons. These results suggest that the interfacial interactions between Ni nanopar-

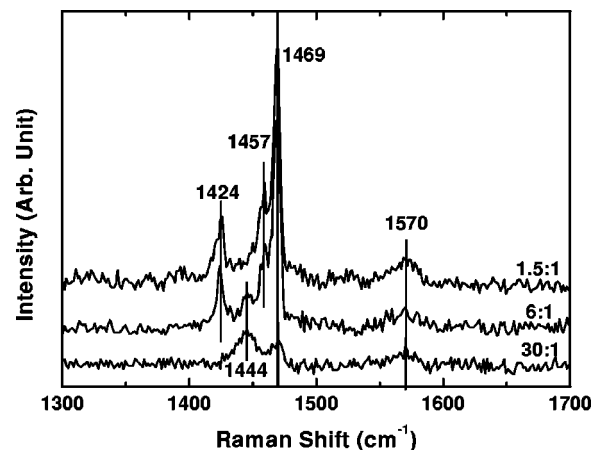


FIG. 3. The Raman spectra of the Ni/ C_{60} films.

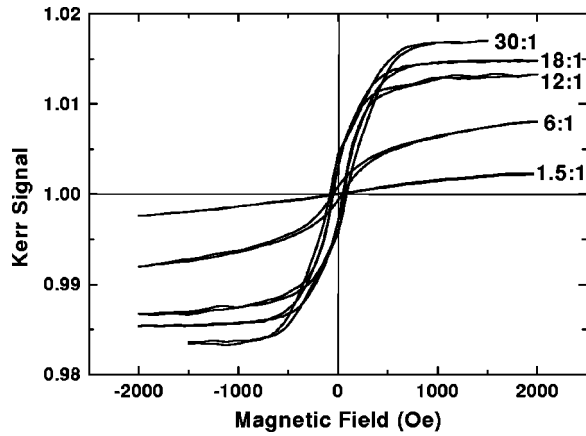


FIG. 4. The hysteresis loops measured by SMOKE systems at room temperature.

ticles and the C_{60} matrix are very strong.

It is interesting to note that the charges transferred from Ni to C_{60} reduce when the Ni nanoparticles become smaller. We think this is due to the quantum size effects of Ni nanoparticles. The average sizes of Ni particles in $N_{Ni}:N_{C60} = 1.5, 6,$ and 30 films are $2.6, 3.3$ and 6.6 nm, respectively (see Table I). For very small metallic nanoparticles, the energy levels become quantized and the number of total free electrons is limited. In this case, their Fermi levels will become lower and lower as more and more electrons are transferred away. When the Fermi level reduces to equal to the lowest unoccupied molecular orbital of the C_{60} molecules, charge transfer from Ni to C_{60} stops. Wang *et al.*¹⁹ studied the interactions between Ag nanoparticles and C_{60} molecules, and concluded that the charge transfer from Ag to C_{60} only occur when the Ag clusters are greater than a critical size (4 nm), while only weak van der Waals type interactions exist between Ag and C_{60} when Ag particles are smaller than 4 nm. This result supports our discussion for Ni/ C_{60} system.

The measurements of magnetic properties were carried out by using a SMOKE instrument with longitudinal configuration, the dc magnetic field being applied is in the in-plane direction and parallel to the incident plane of the He-Ne laser beam. The hysteresis loops measured at room temperature are given in Fig. 4. The loops indicate that the coercivity (H_C) decreases with the decrease of the average particle sizes (see Table I). As the average particle size varied from 3.3 to 2.6 nm, the loop degenerated into a line and H_C reduced from 45 Oe to undetectable. This indicates that the critical size for the superparamagnetic transition lies in between 3.3 and 2.6 nm at room temperature.

It is known that, due to thermal effects, the coercivity of ferromagnetic nanoparticles decreases abruptly with decreasing particle size (D),^{10,20} when the size is less than a critical size (D_{sc}) below which the particle will be a single domain particle. According to Brown's micromagnetic theory,^{21,22} the estimated D_{sc} for a spherical Ni particle is ~ 42 nm. Block *et al.* reported that,¹³ at room temperature, the coercivity of the graphite-coated Ni nanoparticles decreases from ~ 40 to ~ 20 Oe with the decrease of the average particle size from 13.6 to 11.4 nm. However, at room temperature, the

coercivity of $D = 3.3$ nm Ni/ C_{60} film ($N_{Ni}:N_{C60} = 6$) is 45 Oe (see Table I), which is larger than that of $D = 13.6$ nm Ni/C film. Zhao *et al.*¹¹ studied Ni/ SiO_2 granular films, and found that the blocking temperatures (T_B) are 27 K for 3.5 -nm Ni nanoparticles and 80 K for 6.1 -nm nanoparticles. Considering that the superparamagnetic transition size increases with the temperature,²⁰ and that the $D = 3.3$ nm Ni particles in the C_{60} matrix are still in the ferromagnetic state ($H_C = 45$ Oe) for the $N_{Ni}:N_{C60} = 6$ film, we can simply conclude that the transition size of Ni particles in the C_{60} matrix is much smaller than that of Ni nanoparticles in the SiO_2 matrix at room temperature (~ 300 K). Based on the above discussions, we suggest that, for Ni nanoparticles embedded in a C_{60} matrix, the coercivity is enhanced significantly, or in other words, that the critical size of superparamagnetic transition is much smaller as compared to Ni nanoparticles embedded in graphite or SiO_2 matrix.

Coupling between magnetic particles often plays an essential role in determining the magnetic properties of granular systems.²³ However, such coupling reduces with increasing interparticle separation. Murakami *et al.*²⁴ reported that a separation of 1 – 2 nm by SiO_2 layers remarkably weakened the exchange interaction of magnetic grains. Hayashi *et al.*¹² also suggested that 2 -nm-thick graphitelike carbon layers could significantly reduce the exchange coupling between cobalt nanocrystals. Furthermore, Zheng *et al.*⁶ studied the magnetic properties of (Co,Fe,CoFe)/ C_{60} granular films. They suggested that the C_{60} molecules could limit the grain growth and reduce the magnetic coupling between the metal grains. According to our HRTEM results (Fig. 2), Ni nanoparticles distribute in a very narrow size range and are isolated from each other with interparticle separations of ~ 2.5 nm. So we think that the magnetic coupling between Ni nanoparticles should not be the dominant reason for the enhancement of the coercivities in the Ni/ C_{60} films.

In general, bond lengths at the surface of metal nanoparticles tend to contract as an effect of reduced coordination.²⁰ Stadnik *et al.*²⁵ reported that the lattice constant for a 5 -nm Ni particle embedded in a SiO_2 matrix decreases by $\sim 2.4\%$ as compared to the bulk value (2.034 Å). However, in our case, instead of lattice contraction, a lattice expansion of Ni particles was observed (Fig. 1). Pospescu *et al.*²⁶ also reported a lattice expansion of 0.2 – 0.6% for Cu nanoparticles in Cu/ C_{60} granular films. What makes the metal nanoparticles embedded in a C_{60} matrix so different is the strong charge transfers from metal to C_{60} . As electrons are transferred away from a metal nanoparticle, the coupling between the metal atoms is reduced. This will in turn lead to a lattice expansion. The smaller the nanoparticle the less it can offer to the free electrons. For smaller nanoparticles, the ratio of lost electrons to the total number of electrons is higher than that of larger nanoparticles. We think this is the dominant reason why the Ni nanoparticles expands more and more when they become smaller. This kind of lattice expansion may reduce the exchange coupling between Ni atoms, so it tends to disturb the spin orders at the surface of Ni nanoparticles in the Ni/ C_{60} films.

According to Kodama and Berkowitz,¹⁶ when surface

spin disorders are present, the surface anisotropy enhances the coercivities of spinel nanoparticles. When the surface anisotropy is uniaxial, with an axis defined by the dipolar moment of the neighboring ions, the easy axis of these ions is approximately radial. If the spins are perfectly aligned (no surface spin disorder), the effect of the radially symmetric surface anisotropy will average to zero. For this case, Kodama and Berkowitz found that the coercivity was vanishingly small for the 2.5-nm NiFe_2O_4 particle. When there was surface spin disorder, the surface anisotropy no longer averaged to zero, and resulted in an enhanced coercivity (1800 Oe) for the 2.5-nm NiFe_2O_4 particle. Moreover, Nunes *et al.*²⁷ predicted very nonuniform strains in the surface layers of spinel ferrite nanoparticles, with an average expansion of a few percent compared to bulk, in qualitative agreement with x-ray-diffraction data.²⁸ They suggested that such an expansion may result in a stress-induced anisotropy field of up to 70 kOe, which could account for some of the anomalous magnetic behavior of ferrite nanoparticles. Although the objects they considered are ionic materials (NiFe_2O_4 , $\alpha\text{-Fe}_2\text{O}_3$ and CoFe_2O_4), we think their model can be applied to our system in principle. The lattice expansion at the Ni particle surface may also have similar effects of the “broken exchange bond,”¹⁶ reducing the exchange integral²⁷ and leading to surface spin disorder.¹⁶ Furthermore, the spins of the surface nickel atoms may also be perturbed by the surrounding C_{60} molecules and become more difficult to reverse

due to the effect of the interfacial interaction between Ni and C_{60} . Therefore, we suggest that the coercivities are enhanced by the surface anisotropy because of the spin disorder at Ni particle surfaces in a Ni/C_{60} system.

IV. CONCLUSION

In summary, we have studied the size-dependent magnetic properties of Ni nanoparticles in Ni/C_{60} granular films. Ni nanoparticles as small as 3.3 nm still present ferromagnetic properties ($H_C=45$ Oe) at room temperature. The mechanism of the enhancement of coercivities or the reduction of the critical size of superparamagnetic transition is discussed by considering the strong interfacial interaction between Ni particles and the C_{60} matrix. The charge transfer and the lattice expansion may lead to the spin disorder at the surfaces of Ni nanoparticles. Consequently, the surface spin disorder leads to the surface anisotropy and enhances the coercivities of the Ni nanoparticles in the C_{60} matrix.

ACKNOWLEDGMENTS

This work was supported by the NSF of China (50132030, 50121202, 10174073, 19904012) and NKBRFSF (G1999075305), and ICQS of the Chinese Academy of Sciences Foundation.

*Email address: jghou@ustc.edu.cn

¹M. R. C. Hunt, P. Rudolf, and S. Modesti, *Phys. Rev. B* **55**, 7882 (1997).

²B. W. Hoogenboom, R. Hesper, L. H. Tjeng, and G. A. Sawatzky, *Phys. Rev. B* **57**, 11939 (1998).

³J. W. Freeland, K. Bussmann, P. Lubita, Y. U. Idzerda, and C.-C. Kao, *Appl. Phys. Lett.* **73**, 2206 (1998).

⁴Martin Schmidt, Robert Kusche, Bernd von Issendorff, and Hellmut Haberland, *Nature (London)* **393**, 238 (1998).

⁵P. Ball and L. Garwin, *Nature (London)* **355**, 761 (1992).

⁶Lingyi A. Zheng, Bruce M. Lairson, and Enrique V. Barrera, *Appl. Phys. Lett.* **77**, 3242 (2000).

⁷J. G. Hou, Yan Wang, Wentao Xu, S. Y. Zhang, Zou Jian, and Y. H. Zhang, *Appl. Phys. Lett.* **70**, 3110 (1997).

⁸A. F. Hebard, R. R. Ruel, and C. B. Eom, *Phys. Rev. B* **54**, 14 052 (1996).

⁹M. R. C. Hunt, S. Modesti, P. Rudolf, and R. E. Palmer, *Phys. Rev. B* **51**, 10 039 (1995).

¹⁰Chen Chen, Osamu Kitakami, and Yutaka Shimada, *J. Appl. Phys.* **84**, 2184 (1998).

¹¹B. Zhao, Jeff Y. Chow, and X. Yan, *J. Appl. Phys.* **79**, 6022 (1996).

¹²T. Hayashi, S. Hirono, M. Tomita, and S. Umemura, *Nature (London)* **381**, 772 (1996).

¹³J. A. Block, K. Parvin, J. L. Alpers, T. Sezen, and R. LaDuca, *IEEE Trans. Magn.* **34**, 982 (1998).

¹⁴Y. Xu, B. Zhao, and X. Yan, *J. Appl. Phys.* **79**, 6137 (1996).

¹⁵R. H. Kodama, *J. Magn. Magn. Mater.* **200**, 359 (1999).

¹⁶R. H. Kodama and A. E. Berkowitz, *Phys. Rev. B* **59**, 6321 (1999).

¹⁷K. Haneda, *Can. J. Phys.* **65**, 1233 (1986).

¹⁸Y. Maruyama, K. Ohno, and Y. Kawazoe, *Phys. Rev. B* **52**, 2070 (1995).

¹⁹Haiqian Wang, J. G. Hou, O. Takeuchi, Y. Fujisuku, and A. Kawazu, *Phys. Rev. B* **61**, 2199 (2000).

²⁰S. Gangopadhyay, G. C. Hadjipanayis, B. Dale, C. M. Sorensen, K. J. Klabunde, V. Papaefthymiou, and A. Kostikas, *Phys. Rev. B* **45**, 9778 (1992).

²¹W. F. Brown, *Phys. Rev.* **105**, 1479 (1957).

²²Osamu Kitakami, Tomoaki Sakurai, Yoichi Miyashita, Yukio Takeno, Yutaka Shimada, Hisashi Takano, Hiroyuki Awano, Keiichi Ando, and Yutaka Sugita, *Jpn. J. Appl. Phys.* **35**, 1721 (1996).

²³V. Russier, C. Petit, J. Legrand, and M. P. Pileni, *Phys. Rev. B* **62**, 3910 (2000).

²⁴A. Murayama, S. Kondoh, M. Miyamura, in *Proceedings of the 3rd International Symposium on the Physics at Magnetic Materials*, edited by C. S. Kim, T. D. Lee, J. H. Oh (Hamlim, Seoul, Korea, 1995), p. 478.

²⁵Z. M. Stadnik, P. Griesbach, G. Dehe, P. Gütllich, T. Kohara, and G. Stroink, *Phys. Rev. B* **35**, 6588 (1987).

²⁶R. Popescu, D. Macovei, A. Devenyi, R. Manaila, P. B. Barna, A. Kovacs, and J. L. Lábár, *Eur. Phys. J. B* **13**, 737 (2000).

²⁷A. C. Nunes and L. Yang, *Surf. Sci.* **399**, 225 (1998).

²⁸A. C. Nunes and D. Lin, *J. Appl. Crystallogr.* **28**, 274 (1995).